

Cyclohexane as a Li⁺ Selective Ionophore[†]

G. Naresh Patwari[‡] and James M. Lisy*

Department of Chemistry, University of Illinois at Urbana Champaign, Urbana, Illinois 61801

Received: January 30, 2007; In Final Form: May 4, 2007

The M⁺[cyclohexane][Ar] (M = Li, Na, and K) cluster ions were investigated using infrared photodissociation spectroscopy in the C–H stretching region. The alkali metal cation binds to the cyclohexane ring above the ring on the S₆ axis via η³ coordination. The C–H stretching modes are perturbed due to binding of the metal cation and display a significant spread in frequency. The shifts are greatest for the Li⁺ and decrease for Na⁺ and K⁺ with increasing ionic radius. It has been observed that cyclohexane displays greater selectivity for Li⁺ over Na⁺ than the cyclic ether, 12-crown-4. The charge transfer interaction between Li⁺ and cyclohexane is believed to be responsible for the selectivity of Li⁺ over other alkali metal ions.

Introduction

Lithium ion selective ionophores are required for clinical testing of the Li⁺ concentration in the blood serum for the patients undergoing lithium treatment.¹ For clinical testing, the major interference comes from Na⁺ and K⁺ ions, which are also present in the blood. Macrocyclic ethers, such as crown ethers, coronands, and cryptands, have long been used as host molecules for selective binding of metal cations, especially the alkali metal ions.² Several reports exist in the literature wherein macrocyclic molecular hosts have been used to achieve Li⁺ ion selectivity.³ Recently, several nonmacrocyclic host molecules have also been reported, based upon a 1,3,5-triaxially substituted cyclohexane template.⁴ Out of the eight commercially available lithium selective ionophores, half of them contain a cyclohexane ring.⁵ Walkowiak et al. investigated the Li⁺/Na⁺ ion selectivity by solvent extraction in aqueous solutions using lariat ether phosphonic acid monoethyl esters by varying the pendent group.^{3c} Surprisingly, it was found that the selectivity with the cyclohexane as the pendent group was twice as great when compared with 12-crown-4, even though 12-crown-4 is a well-known Li⁺ selective molecular host. In another interesting example, Suzuki et al. have reported the maximum selectivity of 1000 for Li⁺ over Na⁺ when 14-crown-4 was derivatized with two cyclohexane rings.^{3d} In this case, the selectivity was achieved due to encapsulation of Li⁺ by two cyclohexane rings.

Cyclohexane is known to have a negative electrostatic potential above the ring on the S₆ axis, which can influence the binding of a cation to cyclohexane.^{6a} The binding of the alkali metal cations to cyclohexane has been investigated, both experimentally as well as theoretically.^{6,7} Staley and Beauchamp measured the binding energy of Li⁺ with cyclohexane in the gas phase to be 100 kJ mol⁻¹, which is substantial and marginally higher than the binding energy with propene.^{7a} This indicates that for Li⁺ binding, cyclohexane is competitive with the cation–π-interaction. However, from various reports currently available in the literature, it is not very clear as to why cyclohexane binds strongly to Li⁺. Also, the effect of Li⁺ binding on cyclohexane is not known. To resolve these issues, we investigated clusters of cyclohexane (cyH) with the alkali metal ions, viz., Li⁺, Na⁺, and K⁺, using infrared-photodissociation (IRPD) spectroscopy.

Experiment

It is now well established for ionic clusters that argon tagging is a useful technique to lower internal temperature, thus reducing thermal congestion in the vibrational spectra.⁹ The vibrational spectra of single Ar-tagged M⁺[cyH]_{1–2} clusters were recorded using the IRPD technique, described in detail elsewhere.¹⁰ Briefly, the neutral cyH–Ar clusters were formed in a supersonic jet by the expansion of cyH in an argon buffer gas. Alkali metal ions, produced by thermionic emission from a tungsten filament coated with a corresponding salt-enriched suspension of zeolite paste, are injected into the neutral clusters about 30 mm downstream from a 180 μm diameter conical nozzle. The nascent cluster ions stabilize via evaporative cooling. From the ensemble of cluster ions formed in the molecular beam, the species of interest is mass selected using a quadrupole mass filter. These mass-selected cluster ions are then passed to a quadrupole ion guide, where they interact with a tunable infrared laser. The absorption of IR radiation by the cluster ion induces vibrational predissociation to a specific cluster ion fragment, which is monitored using another quadrupole mass filter. The IR spectrum is measured by recording the percent fragmentation as a function of IR frequency. This action spectrum is reported as the predissociation cross section correcting for the laser fluence. The IR source is the idler component of a LiNbO₃ optical parametric oscillator (3 cm⁻¹ bandwidth) pumped by the fundamental of a custom 20 ns Nd:YAG laser (Continuum). Absolute frequency calibration (±2 cm⁻¹) for the spectrum is obtained by measuring the absorption of HCl in a gas cell at 10 Torr. All IR spectra presented here were recorded by monitoring the Ar loss channel, unless specified.

Results and Discussion

The IRPD spectra of M⁺[cyH][Ar] (M = Li, Na, and K) in the C–H stretching region are shown in Figure 1 (traces A–C). Also shown is the IRPD spectrum of Na⁺[H₂O]₄[cyH], recorded using cyH loss channel (trace D), and the gas-phase IR spectrum of bare cyH in the C–H stretching region (trace E) for comparison.¹¹ It is well known that for smaller water clusters the first solvation shell of Na⁺ in the gas phase consists of four water molecules and the fifth ligand triggers the formation of the second solvation shell.¹² In the case of Na⁺[H₂O]₄[cyH], it can be safely assumed that cyH is present in the second solvation shell and is minimally perturbed with respect to bare cyH, as can be seen from traces D and E of Figure 1. In the ensuing discussion, we compare the IRPD spectra of M⁺[cyH][Ar] (M = Li, Na, and K) with the IRPD spectrum of Na⁺[H₂O]₄[cyH].

[†] Part of the “Roger E. Miller Memorial Issue”.

* To whom correspondence should be addressed. E-mail: j-lisy@uiuc.edu.

[‡] Present address: Department of Chemistry, Indian Institute of Technology Bombay, Powai, Mumbai 400 076 India. E-mail: naresh@chem.iitb.ac.in.

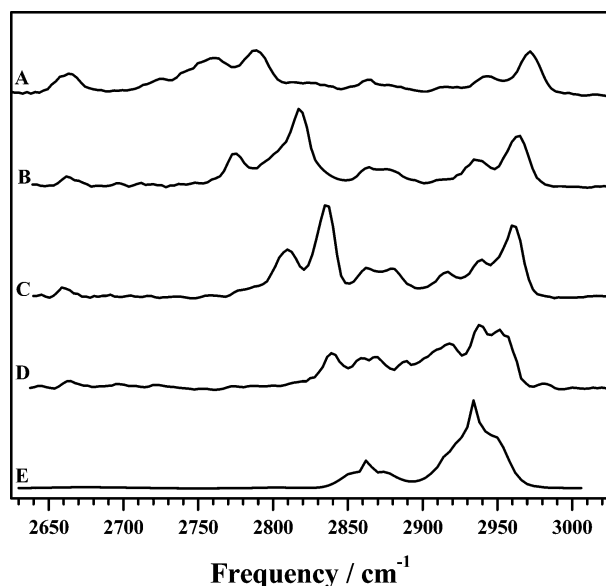


Figure 1. The IRPD spectra of (A) $\text{Li}^+[\text{cyH}][\text{Ar}]$, (B) $\text{Na}^+[\text{cyH}][\text{Ar}]$, (C) $\text{K}^+[\text{cyH}][\text{Ar}]$, (D) $\text{Na}^+[\text{H}_2\text{O}]_4[\text{cyH}]$, and (E) bare cyH in the C–H stretching region.

This comparison can be justified because we are probably observing cyH at similar temperatures in the ion cluster and also the loss of symmetry can be taken into account directly. In the case of $\text{Na}^+[\text{H}_2\text{O}]_4[\text{cyH}]$, several overlapping transitions can be seen in the 2840–2960 cm^{-1} region, corresponding to the C–H stretching vibrations of cyH. The assignment of these transitions to the 12 normal modes arising out of 12 C–H oscillators is not straightforward, as anharmonic and Fermi couplings between the oscillators are expected. Even without a formal assignment, qualitative comparison of the observed features in the IRPD spectra is quite instructive. The binding of cyH with the alkali metal cation above the ring on the S_6 axis (via η^3 coordination) will perturb the C–H oscillators much more than those expected via second solvation shell effects in $\text{Na}^+[\text{H}_2\text{O}]_4[\text{cyH}]$. The IRPD spectra of cyH complexed with all the three ions have roughly the same number of transitions in the C–H stretching region but are spread over a larger range on either side of the spectrum. Further, it can be seen in Figure 1 that in all four cases a feature is observed around 2660 cm^{-1} , which can be assigned to the C–H bend overtone. The increase in the intensity of this band in the order of $\text{Li}^+ > \text{Na}^+ > \text{K}^+$, which is directly related to the proximity of the C–H stretching frequencies in the same order. This Fermi resonance coupling has been similarly observed between the OH stretch and HOH bend overtone in the $\text{X}^+[\text{H}_2\text{O}]$ binary complexes.^{9b} The spread in the C–H stretching frequency range for $\text{Li}^+[\text{cyH}]$ is about 280 cm^{-1} (2710–2990 cm^{-1}) and is larger than that observed for $\text{Na}^+[\text{cyH}]$, 220 cm^{-1} (2760–2980 cm^{-1}), and $\text{K}^+[\text{cyH}]$, 205 cm^{-1} (2770–2975 cm^{-1}). This observed spread in the C–H stretching frequency range suggests that Li^+ interaction with cyH is significantly stronger than the interactions in $\text{Na}^+[\text{cyH}]$ - and $\text{K}^+[\text{cyH}]$.

Shown in Figure 2 are the IRPD spectra of $\text{Li}^+[\text{cyH}]_{1-2}[\text{Ar}]$ and $\text{Na}^+[\text{cyH}]_{1-2}[\text{Ar}]$, which were recorded to observe the capping effect of cyH on the ion. The attachment of the second cyH, as expected, reduces the spread in the frequency range due to increased coordination. Furthermore, the IRPD spectra of the clusters with two cyH moieties have better resolved features, which are due to the lowering of the internal temperatures with the additional cyH. Similar effects were observed in the case of $\text{Cl}^-(\text{CH}_3\text{OH})_{1-3}$ clusters, wherein the shift of the OH stretching frequencies in comparison with bare CH_3OH is reduced with the increase in the number of methanol mol-

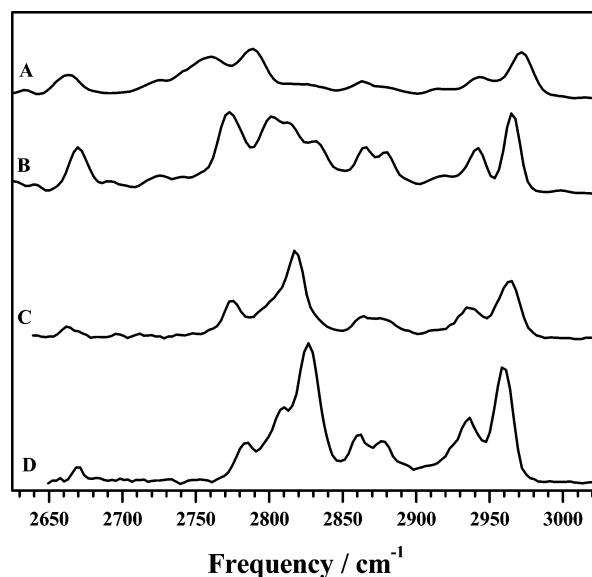


Figure 2. The IRPD spectra of (A) $\text{Li}^+[\text{cyH}][\text{Ar}]$, (B) $\text{Li}^+[\text{cyH}]_2[\text{Ar}]$, (C) $\text{Na}^+[\text{cyH}][\text{Ar}]$, and (D) $\text{Na}^+[\text{cyH}]_2[\text{Ar}]$ in the C–H stretching region.

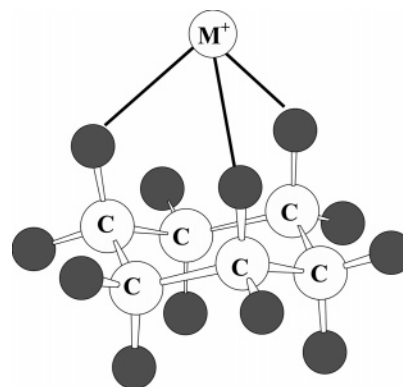


Figure 3. The structure of the $\text{M}^+[\text{cyH}]$ cluster. The M^+-H distances are 1.88, 2.33, and 2.72 Å, for Li^+ , Na^+ , and K^+ , respectively.

TABLE 1: Stabilization Energies (kJ mol^{-1}), Optimized M^+-H and C–H Distances (Å), and CCH Angles (deg) for Various $\text{M}^+[\text{cyH}]$ Complexes Calculated at the MP2/6-311++G(d,p) Level

	ΔE	M^+-H	C–H	$\angle\text{CCH}$
cyH			1.099 ^a , 1.096 ^b	109.1
$\text{Li}^+[\text{cyH}]$	78.6	1.88 (1.96)	1.115 ^c , 1.094 ^d , 1.096 ^e , 1.094 ^f	112.0
$\text{Na}^+[\text{cyH}]$	39.9	2.33 (2.22)	1.110 ^c , 1.095 ^d , 1.097 ^e , 1.095 ^f	110.3
$\text{K}^+[\text{cyH}]$	29.2	2.72 (2.58)	1.107 ^c , 1.095 ^d , 1.097 ^e , 1.096 ^f	109.7

^a Axial. ^b Equatorial. ^c Axial interacting. ^d Equatorial interacting. ^e Axial noninteracting. ^f Equatorial noninteracting. The numbers in the parenthesis are the sum of van der Waal radius of the H atom and the appropriate ionic radius.

ecules.¹³ Even with two cyH moieties attached to the ion, the C–H bend overtone once again can be clearly identified near 2660 cm^{-1} .

To understand the large spread in the C–H stretching frequency range for the $\text{Li}^+[\text{cyH}]$, even in comparison with $\text{Na}^+[\text{cyH}]$ and $\text{K}^+[\text{cyH}]$, we carried out ab initio calculations for the $\text{M}^+[\text{cyH}]$ ($\text{M} = \text{Li}, \text{Na}, \text{and K}$) at MP2/6-311++G(d,p) level, using the Gaussian 98 suite of programs.¹⁴ In each case, a stable minimum was found with the metal ion over the ring bound to three axial hydrogens, as shown in Figure 3. Table 1 lists the binding energies and important geometrical parameters for all three ion clusters. The zero point vibrational energy-corrected binding energies for Li^+ , Na^+ , and K^+ ions binding to the cyclohexane are 78.6, 39.9, and 29.2 kJ mol^{-1} , respectively. The high binding energy of Li^+ to cyclohexane is in

TABLE 2: The Frequencies^a (cm⁻¹) and the Intensities (km mol⁻¹) of the C–H Stretching Vibration of the Cyclohexane Moiety in Bare Cyclohexane and in Its Complexes with Li⁺, Na⁺, and K⁺ Ions

cyH		cyH–Li ⁺		cyH–Na ⁺		cyH–K ⁺	
frequency ^b	intensity	frequency	intensity	frequency	intensity	frequency	intensity
2870 (e _u) <i>2863</i>	84.8	2732 (e)	6.4	2767 (e)	12.7	2800 (e)	11.2
2871 (a _{1g}) <i>2852</i>	0.0	2745 (a ₂)	299.7	2786 (a ₂)	464.3	2814 (a ₂)	405.9
2873 (e _g) <i>2897</i>	0.0	2907 (e)	10.3	2898 (e)	21.5	2894 (e)	28.8
2873 (a _{2u}) <i>2860</i>	66.6	2908 (a ₁)	5.8	2898 (a ₁)	8.1	2894 (a ₁)	11.2
2925 (e _u) <i>2933</i>	168.5	2951 (e)	0.0	2943 (e)	27.2	2940 (e)	44.8
2926 (a _{1g}) <i>2930</i>	0.0	2952 (a ₁)	3.61	2943 (a ₁)	3.1	2940 (a ₁)	11.0
2930 (e _g) <i>2930</i>	0.0	2961 (e)	12.8	2950 (e)	23.1	2944 (e)	20.2
2934 (a _{2u}) <i>2915</i>	116.6	2962 (a ₁)	10.7	2952 (a ₁)	34.4	2948 (a ₁)	58.4

^a The symmetries are given in parenthesis. ^bThe experimental values are given in italics.

TABLE 3: Mulliken, MEP, and NPA Charges on M⁺ in Various M⁺–cyH Complexes, Calculated at the MP2/6-311++G(d,p) Level

	Mulliken	MEP	NPA
Li ⁺ [cyH]	0.738	0.880	0.943
Na ⁺ [cyH]	0.812	0.975	0.983
K ⁺ [cyH]	0.978	0.978	0.995

reasonable agreement with the value reported by Staley and Beauchamp,^{7a} but marginally higher than those reported by Tsuzuki et al., which can be attributed to the difference in the basis sets used.^{6b} It can be inferred from Table 1 that the cyH undergoes substantial change in the geometry, especially in the lengthening of the C–H bonds of the three axial hydrogens bound to the ion. Further, the remaining nine noninteracting C–H bonds are affected and exhibit a slight contraction in bond length. The elongation of the interacting axial C–H bonds and the contraction of the noninteracting C–H bonds is in the order of Li⁺ > Na⁺ > K⁺. This implies that the most red-shifted transitions observed in Figure 1 (traces A–C) can be attributed to the stretching vibrations of the interacting axial CH bonds. Additionally, the blue-shifted transitions can be attributed to the noninteracting CH bonds. The M⁺ ion to axial hydrogen distances for Li⁺, Na⁺, and K⁺ are 1.88, 2.33, and 2.72 Å, respectively. In the case of Li⁺[cyH] cluster, the ion hydrogen distance is less than the sum of the ionic radius of Li⁺ and van der Waals radius of hydrogen, while for Na⁺ and K⁺ the distance is larger. Additionally, the CCH angle opens up by almost 3 degrees to accommodate the Li⁺ ion, while the corresponding changes for the Na⁺ and K⁺ ions are substantially smaller. These changes indicate a much stronger interaction between cyH and Li⁺ in comparison with Na⁺ and K⁺ and are in accord with the binding energies. Further, Table 2 lists the calculated vibrational frequencies of bare cyH and the three M⁺[cyH] (M = Li, Na, and K) complexes (scaling factor 0.941), which qualitatively agree with the fact that the CH-stretching region of the cyH moiety spreads out in the presence of the ion with the maximal spread occurring for the Li⁺ complex.

The IRPD spectra and the ab initio calculations predict a strong interaction between the Li⁺ and the cyH. Because in all the three cases the bare ion is interacting with the cyH, it is reasonable to assume that the charge transfer might be the dominant criterion for the stabilization of the Li⁺ complex. It is well known that Mulliken charges are not always adequate to explain bonding in various situations. Therefore, molecular electrostatic potential (MEP) derived charges as well as charges from the natural population analysis (NPA) were also calculated for all the three cluster ions at the MP2/6-311++G(d,p) level and are presented in Table 3. In all three cases, MEP estimates marginally higher charge transfer than NPA. However, the trend in analyses indicates that the residual charge on Li⁺ is substantially lower than for Na⁺ and K⁺ in their respective complexes with cyH. These results clearly indicate that the primary nature of interaction between Li⁺ and cyH is through charge transfer. Further, it can be expected that the pairwise (M⁺–cyH) interaction is lowered with increased coordination

TABLE 4: Calculated Stabilization Energies (kJ mol⁻¹) for Various Alkali Metal Ion Complexes at the MP2/6-311++G(d,p) Level

	Li ⁺	Na ⁺	K ⁺
water	139.9	96.6	73.6
ammonia	159.7	109.1	79.1
cyH	78.6	39.9	29.2
ethylene	80.9	50.2	33.9
methane	46.6	22.6	13.9
12-crown-4 ^a	377	255	193

^a Experimental binding energies from ref 14.

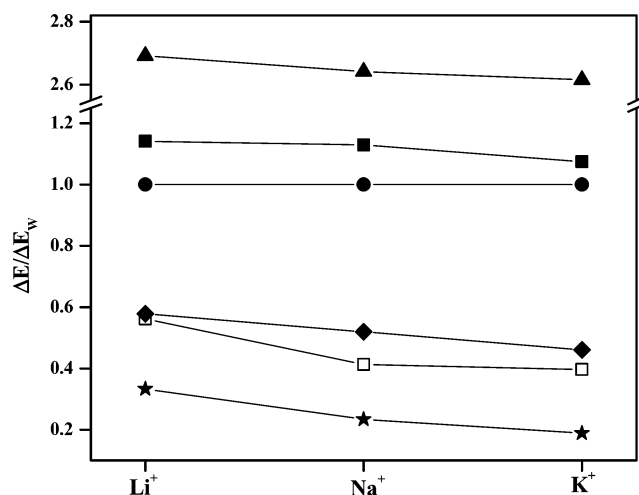


Figure 4. The plot showing the binding energies of Li⁺, Na⁺, and K⁺ to various ligands (▲ 12-crown-4; ■ ammonia; □ cyH; ◆ ethylene; ★ methane) relative to the binding of the respective ion with water (●). The binding energies for all the complexes were calculated at the MP2/6-311++G(d,p) level, while those of 12-crown-4 were taken from ref 14.

and thus is leading to a lower amount of charge transfer from M⁺ to cyH in the M⁺[cyH]₂ complexes. This will lead to smaller shifts in the C–H stretching vibrations in the M⁺[cyH]₂ complexes in comparison with M⁺[cyH]₂ complexes, as observed in Figure 2.

The strong association of cyH with Li⁺ compared to other alkali metal ions such as Na⁺ and K⁺ might be one of the major contributing factors for the incorporation of the cyclohexyl ring in the commercially available lithium selective ionophores. To assess the Li⁺ selectivity by cyH, the binding energies of some simple molecules such as water, ammonia, ethylene, methane with Li⁺, Na⁺ and K⁺ were calculated at MP2/6-311++G(d,p) level of the theory, and are listed in Table 4. Furthermore, the experimental gas-phase-binding energies of 12-crown-4 with the three alkali ions are also listed for comparison.¹⁵ An interesting observation can be made from Table 4 in that the binding energies of Li⁺ ion to cyH and ethylene are comparable, while the other two ions (Na⁺ and K⁺) bind much more strongly to ethylene than with cyH. This implies that Li⁺[cyH] binding is competitive with the Li⁺–π-interaction. Figure 4 shows the plot

of binding energies of various ligands to the three alkali metal cations, relative to water. If one assumes that water is not selective toward any of the alkali metal ions, then the plot clearly indicates that selectivity of cyH toward Li^+ is much more pronounced than any other ligand including the bare 12-crown-4. The bare 12-crown-4 has marginal selectivity toward Li^+ over Na^+ , even though it is well known as Li^+ selective ionophore in aqueous media. The difference may be because of the cooperative effect between the binding of the metal ion and the water structure around it in the aqueous environment. The ability of bare cyH to preferentially bind to Li^+ ion over other alkali metal ions can be effectively used to design Li^+ selective ionophores. The fact that out of eight commercially available Li^+ selective ionophores, half of them contain the cyH ring may not be a coincidence and is a testimonial for the ability of cyH to bind selectively to Li^+ .

Conclusions

The IRPD spectra of $\text{M}^+[\text{cyH}]$ ion complexes reveal that Li^+ perturbs the C–H oscillators of the cyclohexane ring much more strongly than Na^+ and K^+ . Ab initio calculations indicate that the binding of Li^+ to cyclohexane is comparable with the Li^+ – π -interaction. Charge analysis points out that charge transfer is the dominant factor stabilizing the interaction of Li^+ with cyclohexane. Comparison of the binding energy of various ligands to the three alkali metal cations, including 12-crown-4, relative to water clearly highlights that cyclohexane has pronounced ability to selectively bind to Li^+ ion.

Acknowledgment. The authors thank the National Science Foundation (U.S.) for partial support of this research through grants CHE 00-72178 and CHE 04-15859 (to J.M.L.).

References and Notes

- (1) (a) Soares, J. C.; Gershon, S. *Neuropsychopharmacology* **1998**, *19*, 167–182. (b) Friedrich, M. J. *JAMA, J. Am. Med. Assoc.* **1999**, *281*, 2271–2273. (c) Tosteson, D. C. *Sci. Am.*, **1981**, *244*, 164.
- (2) Izatt, R. M.; Pawlak, K.; Bradshaw, J. S.; Bruening, R. L. *Chem. Rev.* **1995**, *95*, 2529–2586. (b) Izatt, R. M.; Bradshaw, J. S.; Pawlak, K.; Bruening, R. L.; Taret, B. J. *Chem. Rev.* **1992**, *92*, 1261–1354. (c) Izatt, R. M.; Pawlak, K.; Bradshaw, J. S.; Bruening, R. L. *Chem. Rev.* **1991**, *91*, 1721–2085. (d) Izatt, R. M.; Bradshaw, J. S.; Nielsen, S. A.; Lamb, J. D.; Christensen, J. J.; Sen, D. *Chem. Rev.* **1985**, *85*, 271–339.
- (3) Cram, D. J.; Kaneda, T.; Helgeson, R. C.; Brown, S. B.; Knobler, C. B.; Maverick, E.; Trueblood, K. N. *J. Am. Chem. Soc.* **1985**, *107*, 3645–3657. (b) Piotrowski, H.; Severin, K. *Proc. Natl. Acad. Sci. U.S.A.* **2002**, *99*, 4997–5000. (c) Walkowiak, W.; Ndip, G.; Bartsch, R. A. *Anal. Chem.* **1999**, *71*, 1021–1026. (d) Suzuki, K.; Yamada, H.; Sato, K.; Watanabe,

- (e) Hisamoto, H.; Tobe, Y.; Kobihiro, K. *Anal. Chem.* **1993**, *65*, 3404–3410. (f) Kang, Y. R.; Lee, K. Y.; Nam, H.; Cha, G. S.; Jung, S. O.; Kim, J. S. *Analyst*, **1997**, *122*, 1445–1450. (g) Metzger, E.; Dohner, R.; Simon, W.; Vonderschmitt, D. J.; Gautschi, K. *Anal. Chem.* **1987**, *59*, 1600–1603. (h) Katakay, R.; Nicholson, P. E.; Parker, D.; Covington, A. K. *Analyst*, **1991**, *116*, 135–140.
- (4) (a) Paquette, L. A.; Tae, J. *J. Am. Chem. Soc.* **2001**, *123*, 4974–4984. (b) Paquette, L. A.; Tae, J.; Hickey, E. R.; Rogers, R. D. *Angew. Chem., Int. Ed.* **1999**, *38*, 1409–1411. (c) McGarvey, G. J.; Stepanian, M. W.; Bressette, A. R.; Sabat, M. *Org. Lett.* **2000**, *2*, 3453–3456. (d) Hegetschweiler, K. *Chem. Soc. Rev.* **1999**, *28*, 239–249.
- (5) Fluka Selectophore Catalogue. Fluka, Buchs, Switzerland, 1991. <http://www.sigmaaldrich.com/img/assets/5100/26LITHIU.pdf> (accessed Oct 2006).
- (6) (a) Gadre, S. R.; Pingale, S. S. *J. Am. Chem. Soc.* **1998**, *120*, 7056–7062. (b) Tsuzuki, S.; Yoshida, M.; Uchimar, T.; Mikami, M. *J. Phys. Chem. A* **2001**, *105*, 769–773.
- (7) (a) Staley, R. H.; Beauchamp, J. L. *J. Am. Chem. Soc.* **1975**, *97*, 5920–5921. (b) Eller, K.; Schwarz, H. *Chem. Rev.* **1991**, *91*, 1121–1177.
- (8) (a) Mecozzi, S.; West, A. P., Jr.; Dougherty, D. A. *Proc. Natl. Acad. Sci. U.S.A.*, **1996**, *93*, 10566–10571. (b) Kim, D.; Hu, S.; Tarakeshwar, P.; Kim, K. S.; Lisy, J. M. *J. Phys. Chem. A* **2003**, *107*, 1228–1238. (c) Kim, K. S.; Tarakeshwar, P.; Lee, J. Y. *Chem. Rev.* **2000**, *100*, 4145–4186.
- (9) Ayotte, P.; Bailey, C. J.; Kim, J.; Johnson, M. A. *J. Chem. Phys.* **1998**, *108*, 444–449. (b) Ayotte, P.; Weddle, G. H.; Kim, J.; Johnson, M. A. *J. Am. Chem. Soc.* **1998**, *120*, 12361–12362. (c) Vaden, T. D.; Forinash, B.; Lisy, J. M. *J. Chem. Phys.* **2002**, *117*, 4628–4631. (d) Vaden, T. D.; Weinheimer, C. J.; Lisy, J. M. *J. Chem. Phys.* **2004**, *121*, 3102–3107.
- (10) (a) Weinheimer, C. J.; Lisy, J. M. *J. Phys. Chem.* **1996**, *100*, 15305–15308. (b) Weinheimer, C. J.; Lisy, J. M. *Chem. Phys.* **1998**, *239*, 357–368. (c) Vaden, T. D.; Weinheimer, C. J.; Lisy, J. M. *J. Chem. Phys.* **2004**, *121*, 3102–3107. (d) Lisy, J. M. *J. Chem. Phys.* **2006**, *125*, 133302/1–132302/19.
- (11) NIST chemistry webbook. <http://webbook.nist.gov/chemistry/> (accessed April 2007).
- (12) Patwari, G. N.; Lisy, J. M. *J. Chem. Phys.* **2003**, *118*, 8555–8558.
- (13) Cabarcos, O. M.; Weinheimer, C. J.; Martinez, T. J.; Lisy, J. M. *J. Chem. Phys.* **2003**, *110*, 9516–26.
- (14) Frisch, M. J.; Trucks, G. W.; Schlegel, H. B.; Scuseria, G. E.; Robb, M. A.; Cheeseman, J. R.; Zakrzewski, V. G.; Montgomery, J. A., Jr.; Stratmann, R. E.; Burant, J. C.; Dapprich, S.; Millam, J. M.; Daniels, A. D.; Kudin, K. N.; Strain, M. C.; Farkas, O.; Tomasi, J.; Barone, V.; Cossi, M.; Cammi, R.; Mennucci, B.; Pomelli, C.; Adamo, V.; Clifford, S.; Ochterski, J.; Petersson, G. A.; Ayala, P. Y.; Cui, Q.; Morokuma, K.; Malick, D. K.; Rabuck, A. D.; Raghavachari, K.; Foresman, J. B.; Cioslowski, J.; Ortiz, J. V.; Baboul, A. G.; Stefanov, B. B.; Liu, G.; Liashenko, A.; Piskorz, P.; Komaromi, I.; Gomperts, R.; Martin, R. L.; Fox, D. J.; Keith, T.; Al-Laham, M. A.; Peng, C. Y.; Nanayakkara, A.; Challacombe, M.; Gill, P. M. W.; Johnson, B.; Chen, W.; Wong, M. W.; Andres, J. L.; Gonzalez, C.; Head-Gordon, M.; Replogle, E. S.; Pople, J. A. *Gaussian 98*, Revision A.9; Gaussian, Inc.: Pittsburgh PA, 1998.
- (15) More, M. B.; Glendening, E. D.; Ray, D.; Feller, D.; Armentrout, P. B. *J. Phys. Chem.* **1996**, *100*, 1605–1614. (b) Hill, S. E.; Glendening, E. D.; Feller, D. *J. Phys. Chem. A* **1997**, *101*, 6125. (c) More, M. B.; Ray, D.; Armentrout, P. B. *J. Phys. Chem. A* **1997**, *101*, 831–839.